Long-Range Forces in Meson-Baryon Systems*

E. GOLOWICH†
Laboratory of Nuclear Studies, Cornell University, Ithaca, New York
(Received 12 April 1965)

We have evaluated single-particle-exchange forces at low energies for all two-particle meson-baryon states with angular momentum from $S_{1/2}$ to $H_{11/2}$. Using real masses and $SU(3)$ coupling constants normalized to experiment, we considered the exchange of the following $SU(3)$ multiplets: baryon octet, $P_{3/2}$ decuplet, $Y_0^*(1520)$ singlet, vector-meson octet (vector and tensor coupling), and $D_{3/2}$ octet. The forces were classified in the direct channel according to $SU(3)$ irreducible representations, an association which is inexact owing to mass splitting but which nevertheless allows us to relate resonant states thereby generated in various isospin and hypercharge channels. We found strong attractive forces in the $P_{1/2},F_{5/2}$ octet, $P_{3/2},F_{7/2}$ decuplet, and $D_{3/2}$ singlet states. In particular, the exchange of vector mesons was observed to play a significant role in all these channels. Our analysis suggests that the $D_{5/2}$ $Y_1^*(1765)$ be assigned to an octet, the other members of which are relatively inhibited by mass-splitting effects to the extent that they may not be observable experimentally as resonances. No forces likely to generate resonances in the multiplet **27** were found.

1. INTRODUCTION

SCATTERING experiments performed in the past five years have shown that the system of strongly interacting particles contains a notable amount of structure. Not only do the data exhibit the presence of many bound states and resonances, but when each such state is defined in terms of a set of quantum numbers, the system is found to have a strikingly systematic appearance. We examine these effects by presenting in this paper a multichannel analysis of low-energy meson-baryon elastic scattering. This is done by deriving expressions for and studying the properties of long-range single-particle-exchange forces which we take to constitute an important part of the low-energy dynamics. Although we make use of the language of dispersion relations to do this, our approach can essentially be summarized by the following set of rules and assumptions:

(1) Use Lorentz invariance to decompose the scattering amplitude into invariant functions.

(2) Represent a particle by a pole in the scattering amplitude, the location and residue of which are determined by the particle mass and coupling constant, respectively.

(3) Assume a continuation of the amplitude away from this pole to the physical regions of the crossed channels.

Using real masses and $SU(3)$ coupling constants normalized to experiment, we determine Born phase shifts $\delta^B(W)$ in the direct-channel [see Figure 1(a)] partial-wave states $j=0+$, $1\pm$, $2\pm$, $3\pm$, $4\pm$, $5\pm$ (where $j=l\pm\frac{1}{2}$) at center-of-mass energies W such that $|\delta^B(W)|<1$ radian. This analysis constitutes merely the first step in a complete dispersion-theoretic calculation of a scattering amplitude. However, such an ambitious project is beset by the twin difficulties of (i) lack of knowledge of how long- and short-range forces behave at energies far above threshold and (ii) imposing unitarity correctly, the number of open channels increasing without limit as energy becomes arbitrarily large. Therefore, although limiting ourselves to conclusions of qualitative or at best semiquantitative nature, we work in a kinematical region where we are relatively confident of the important forces, and where a multichannel treatment is well within reach.

We express the various kinematical relations relevant to this problem in Sec. 2 and derive expressions for forces in Sec. 3. Several important details of the derivation are considered in Sec. 4 and various applications are treated in Sec. 5.

2. KINEMATICS

The reactions we consider in this paper are of the type shown schematically in Fig. 1(a). The quantum numbers (p,M_i,a), (q,m_i,b) describe the initial baryon and meson, and (p',M_f,c), (q',m_f,d) the final baryon and meson where, in particular, for the initial baryon, p = four-momentum in center-of-mass frame, M_i = mass, and a = all other relevant quantum numbers, and similarly for the other particles. The unitary scattering matrix S connecting the initial state (i) to the final state (f) may be expressed in terms of the transition matrix T,

$$S_{fi}=\delta_{fi}+i(2\pi)^4\delta^{(4)}(p+q-p'-q')\times\left(\frac{E_iE_f}{4\omega_i\omega_fM_iM_f}\right)^{1/2}T_{fi}\quad(1)$$

and T may be decomposed into two Lorentz-invariant amplitudes A, B by[1]

$$T=A+\tfrac{1}{2}(q+q')\cdot\gamma B.\quad(2)$$

* This work constitutes a section of the thesis submitted by the author to Cornell University in partial fulfillment of the requirements for a Ph.D.

† Supported by a National Science Foundation Fellowship.

[1] P. T. Matthews, *Lectures on Strong Interactions* (W. A. Benjamin, Inc., New York, 1964), gives a derivation of the relevant kinematics. Our metric is $x\cdot y=x_0y_0-\mathbf{x}\cdot\mathbf{y}$ and we adopt the convention for γ matrices given in S. Schweber, *Introduction to Relativistic Quantum Field Theory* (Row, Peterson and Company, Evanston, Illinois, 1961). We take $\hbar=c=1$.

We further define amplitudes related to the phase shift in the $j=l\pm\frac{1}{2}$ angular-momentum state, letting $k_i=|\mathbf{p}|=|\mathbf{q}|$, $k_f=|\mathbf{p}'|=|\mathbf{q}'|$:

$$f_{l\pm}=\frac{e^{i\delta_{l\pm}}\sin\delta_{l\pm}}{k_i^{1/2}k_f^{1/2}}, \tag{3}$$

and the differential scattering cross section in the center-of-mass system:

$$\frac{d\sigma}{d\Omega}=\frac{k_f}{k_i}\sum_{\text{spins}}|\langle f|f_1+(\boldsymbol{\sigma}\cdot\hat{q}')(\boldsymbol{\sigma}\cdot\hat{q})f_2|i\rangle|^2, \tag{4}$$

where, if x is the cosine of the scattering angle,

$$f_1=\sum_l[f_{l+}P_{l+1}'(x)-f_{l-}P_{l-1}'(x)],$$
$$f_2=\sum_l(f_{l-}-f_{l+})P_l'(x), \tag{5a}$$

$$f_{l\pm}=\frac{1}{2}\int_{-1}^{1}dx[f_1P_l(x)+f_2P_{l\pm1}(x)]. \tag{5b}$$

The amplitudes f_1, f_2 are expressed as functions of A, B by

$$\begin{pmatrix}f_1\\f_2\end{pmatrix}=\alpha\begin{pmatrix}A\\B\end{pmatrix};\quad \alpha=\frac{1}{2W}\begin{bmatrix}[(E_i+M_i)(E_f+M_f)]^{1/2} & \left(W-\frac{M_i+M_f}{2}\right)[(E_i+M_i)(E_f+M_f)]^{1/2}\\ -[(E_i-M_i)(E_f-M_f)]^{1/2} & \left(W+\frac{M_i+M_f}{2}\right)[(E_i-M_i)(E_f-M_f)]^{1/2}\end{bmatrix}, \tag{6}$$

where W is the total energy in the center-of-mass system, which we shall measure in units of the pion mass μ, and E is the baryon energy

$$E(W)=(W^2+M^2-m^2)/2W. \tag{6a}$$

It is appropriate that we now introduce the concept of crossing into the discussion by considering several more kinematical relations suitable for describing the reactions

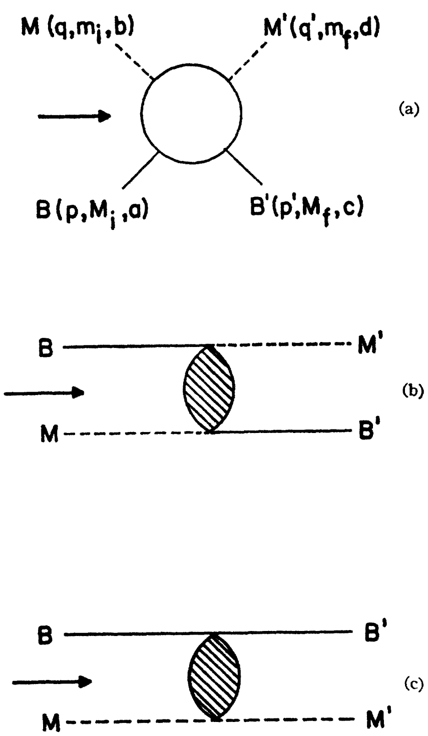

FIG. 1. (a) The process under consideration in this paper: a meson M and baryon B scatter in the s channel elastically into a meson M' and baryon B'. (b), (c) Diagrammatical representation of single-particle exchange forces generated by u- and t-channel processes, respectively.

$$P+B\to P'+B', \tag{7a}$$
$$B+\bar{B}'\to P'+\bar{P}, \tag{7b}$$
$$B+\bar{P}'\to B'+\bar{P}. \tag{7c}$$

A bar denotes an antiparticle, and B, P are a baryon and meson, respectively. We let

$$s=(p+q)^2, \tag{8a}$$
$$t=(p-p')^2, \tag{8b}$$
$$u=(p-q')^2, \tag{8c}$$

represent the square of the invariant energy in the center-of-mass system of the reactions 7(a), (b), and (c), respectively. The momentum in the reaction 7(a), the direct channel, is

$$k^2=W^2/4-\tfrac{1}{2}(M^2+m^2)+(M^2-m^2)^2/4W^2 \tag{9}$$

and the quantities t, u are related to direct-channel parameters by

$$t=-2k_ik_f\left(\frac{2E_iE_f-M_i^2-M_f^2}{2k_ik_f}-x\right), \tag{10a}$$

$$u=m_i^2+m_f^2-W^2+2E_iE_f-2k_ik_fx. \tag{10b}$$

The dynamical information about meson-baryon scattering is completely described by the invariant amplitudes A, B. We assume that each of these satisfies the Mandelstam representation,[2] which describes their singularity content and crossing properties. In particular, we wish to find expressions for forces in a state of

[2] S. Mandelstam, Phys. Rev. **112**, 1344 (1958).

definite angular momentum, and so we study the partial-wave projections[3,4]

$$\begin{pmatrix}A_l\\B_l\end{pmatrix}=\frac{1}{2}\int_{-1}^{1}dx\begin{pmatrix}A\\B\end{pmatrix}P_l(x). \tag{11}$$

3. DERIVATION OF EXPRESSIONS FOR LONG-RANGE FORCES

One generally writes[5] dispersion relations by fixing the energy (fixed s) or the momentum transfer (fixed t). We choose to use fixed-s dispersion relations in the following derivations, delaying a discussion of the significance of this choice until the next section. In order to determine forces generated by u-channel processes, we define amplitudes $A^u(s,t)$, $B^u(s,t)$ by

$$\begin{pmatrix}A^u(s,t)\\B^u(s,t)\end{pmatrix}=\frac{1}{\pi}\int^{\infty}\frac{du'}{u'-u}\,\mathrm{Im}\begin{pmatrix}A(u',t)\\B(u',t)\end{pmatrix}, \tag{12}$$

where (i) we momentarily ignore isospin crossing relations, (ii) the lower limit on the integral includes all bound states in the u channel, a device which treats bound states and resonances equivalently in order to keep the angular-momentum bookkeeping to a minimum, (iii) the variable t inside the integral is a brief way of expressing $(M_i^2+M_f^2+m_i^2+m_f^2-s-u')$, since the variable s must be kept fixed. We write (12) in terms of the amplitudes f_1, f_2 by using (6),

$$\begin{pmatrix}f_1\\f_2\end{pmatrix}=\frac{1}{\pi}\int^{\infty}\frac{du'}{u'-u}\mathbf{D}(s,u')\,\mathrm{Im}\begin{pmatrix}f_1\\f_2\end{pmatrix}, \tag{13}$$

$$\mathbf{D}(s,u')=\frac{1}{2W}\begin{bmatrix}\left(\frac{(E_i+M_i)(E_f+M_f)}{(E_i'+M_i)(E_f'+M_f)}\right)^{1/2}(M_i+M_f+u'^{1/2}-W) & \left(\frac{(E_i+M_i)(E_f+M_f)}{(E_i'-M_i)(E_f'-M_f)}\right)^{1/2}(M_i+M_f-u'^{1/2}-W)\\ \left(\frac{(E_i-M_i)(E_f-M_f)}{(E_i'+M_i)(E_f'+M_f)}\right)^{1/2}(-M_i-M_f-u'^{1/2}-W) & \left(\frac{(E_i-M_i)(E_f-M_f)}{(E_i'-M_i)(E_f'-M_f)}\right)^{1/2}(u'^{1/2}-M_i-M_f-W)\end{bmatrix} \tag{14}$$

where the primed and unprimed quantities refer to the u' and s channels, respectively. From (10b),

$$u'-u=-2k_ik_f(y-x),\qquad y=\frac{m_i^2+m_f^2+2E_iE_f-u'-W^2}{2k_ik_f}, \tag{15}$$

and expanding $(y-x)$ in terms of Legendre functions of the first and second kinds,[6]

$$(y-x)^{-1}=\sum_{n=0}^{\infty}(2n+1)Q_n(y)P_n(x), \tag{16}$$

we obtain

$$\begin{pmatrix}f_1\\f_2\end{pmatrix}=\frac{-1}{2\pi k_ik_f}\int du'\sum_{n=0}^{\infty}(2n+1)P_n(x)Q_n(y)\times\left\{\begin{pmatrix}D_{11}\\D_{21}\end{pmatrix}\mathrm{Im}f_1+\begin{pmatrix}D_{12}\\D_{22}\end{pmatrix}\mathrm{Im}f_2\right\}. \tag{17}$$

If we know the *full amplitudes* in the u channel, (17) gives the resulting force in the direct channel. Now, part of our basic assumption is that the strongly interacting particles be dynamically equivalent entities described by a self-consistent set of amplitudes. We can get a semiquantitative check on this by finding the forces generated in the direct channel by *bound states* and *resonances* in crossed channels, since these quantities presumably dominate the amplitudes at low energies. If we consider a particle of mass M and spin $j=l'\pm\frac{1}{2}$ in the u channel, then from (5a),

$$f_1(u',t)=\pm P_{l'\pm1}'(x_u)f_{l'\pm}(u'),\qquad f_2(u',t)=\mp P_{l'}'(x_u)f_{l'\pm}(u') \tag{18}$$

where the prime on the Legendre polynomials $P_{l'}(x_u)$, $P_{l'\pm1}(x_u)$ refers to differentiation with respect to the angle of scattering in the u channel,

$$x_u=(t+2E_i^uE_f^u-M_i^2-M_f^2)/2k_i^uk_f^u. \tag{19}$$

We next make the sharp-resonance approximation,

$$\mathrm{Im}f_{l'\pm}(u')=\pi\frac{\Gamma_{ir}^{1/2}\Gamma_{fr}^{1/2}}{k_{ir}^{1/2}k_{fr}^{1/2}}W_r\delta(u'-M^2) \tag{20}$$

which yields a Breit-Wigner form upon insertion into a dispersion relation. The subscripts r imply evaluation at the resonant energy, and the quantities Γ_{ir}, Γ_{fr} may be considered decay widths into the initial and final states, respectively. Use of (20) means that we are treating the particles as having no structure, so that in this approximation, our forces are equivalent to those found in lowest order renormalized perturbation theory with a particular choice of propagator.

[3] S. Frautschi and J. Walecka, Phys. Rev. **120**, 1486 (1960).
[4] W. Frazer and J. Fulco, Phys. Rev. **119**, 1420 (1960).
[5] Our approach is similar to that presented in P. Carruthers, Phys. Rev. **133**, B497 (1964).
[6] E. Whittaker and G. Watson, *Modern Analysis* (Cambridge University Press, New York, 1952), 4th ed., p. 321.

Upon performing the u' integration,

$$\begin{pmatrix} f_1 \\ f_2 \end{pmatrix} = \frac{\Gamma_{ir}^{1/2}\Gamma_{fr}^{1/2}}{2k_{ir}^{1/2}k_{fr}^{1/2}} \frac{W_r}{k_i k_f} \sum_{n=0}^{\infty} (2n+1) P_n(x) Q_n(y) \left\{ \begin{pmatrix} D_{11} \\ D_{21} \end{pmatrix} (\mp P_{l'\pm1}'(x_u)) + \begin{pmatrix} D_{12} \\ D_{22} \end{pmatrix} (\pm P_{l'}'(x_u)) \right\}, \tag{21}$$

and applying (5b), we come to the result,

$$f_{l\pm}(s) = \frac{\Gamma_{ir}^{1/2}\Gamma_{fr}^{1/2}}{2k_{ir}^{1/2}k_{fr}^{1/2}} \frac{W_r}{k_i k_f} \{ [D_{11}(s,M)(\mp P_{l'\pm1}') + D_{12}(s,M)(\pm P_{l'}')] Q_l(y)$$
$$+ [D_{21}(s,M)(\mp P_{l'\pm1}') + D_{22}(s,M)(\pm P_{l'}')] Q_{l\pm1}(y) \}. \tag{22}$$

Next, we indicate the approach needed to find a general expression for the forces generated by processes in the direct t channel. Since helicity amplitudes F_{++}, F_{+-} are generally used to describe the annihilation reactions which take place in the t channel, we relate them to the invariant amplitudes A,B, letting q_i,q_f be the center-of-mass momenta of the reaction $PP \to B\bar{B}'$, and z_t be the cosine of the scattering angle;

$$\begin{pmatrix} A \\ B \end{pmatrix} = \mathbf{C} \begin{pmatrix} F_{++} \\ F_{+-} \end{pmatrix}; \quad \mathbf{C} = \begin{bmatrix} \left(\frac{t}{q_i^2}\right)^{1/2} (-8\pi) & \frac{-(M_i+M_f) z_t (-8\pi)}{q_i (1-z_t^2)^{1/2}} \\ 0 & \frac{16\pi}{(1-z_t^2)^{1/2}} \end{bmatrix}. \tag{23}$$

The helicity amplitudes may be decomposed into partial waves ($T^J \equiv |JM;\lambda_1\lambda_2\rangle$),

$$F_{++} = \frac{1}{q_f} \sum_J (J+1/2) T_+^J P_J(z_t),$$
$$F_{+-} = \frac{(1-z_t^2)^{1/2}}{q_f} \sum_J \frac{(J+1/2)}{[J(J+1)]^{1/2}} T_-^J P_J'(z_t), \tag{24}$$

where

$$T^J = -i \left(\frac{q_f}{q_i}\right)^{1/2} S^J, \tag{25}$$

and may also be related to the angular momentum states, $|JM;LS\rangle$;

$$|JM;\lambda_1\lambda_2\rangle = \sum_L \langle JM;LS|JM;\lambda_1\lambda_2\rangle |JM;LS\rangle. \tag{26}$$

From Jacob and Wick,[7]

$$\langle JM;LS|JM;\lambda_1\lambda_2\rangle = \left(\frac{2L+1}{2J+1}\right)^{1/2} C(LSJ;0\lambda) C(s_1 s_2 s;\lambda_1-\lambda_2). \tag{27}$$

Equations (27), (26), (24), and (23) can be used to find resonant forms for the invariant amplitudes A, B which then lead to expressions for forces. In fact, we shall only be interested in forces generated by vector mesons, for which we now go through the above procedure in somewhat more detail. The only possible resonant states are S and D waves, so representing these states by β_S, β_D, we obtain

$$T_+^{j=1} = (\tfrac{3}{2})^{1/2} \left(\frac{q_i}{q_f}\right)^{1/2} \left(\frac{\beta_S - \sqrt{2}\beta_D}{3}\right)$$
$$T_-^{j=1} = (\tfrac{3}{2})^{1/2} \left(\frac{q_i}{q_f}\right)^{1/2} \left(\frac{\sqrt{2}\beta_S + \beta_D}{3}\right). \tag{28}$$

Since one determines the vector-meson–baryon coupling strength from the residues of pole fits, $\Gamma_i(t)$, to form factor data, we combine (28) with Eq. (3.17) in Ref. 8 to yield the more convenient expressions,

$$T_+^{j=1} = -t^{1/2} \frac{(M_i+M_f)}{2} q_i^2 \left[\frac{\Gamma_1(t)}{\frac{1}{4}t} + \frac{\Gamma_2(t)}{\frac{1}{2}(M_i+M_f)} \right],$$
$$T_-^{j=1} = -\sqrt{2} \frac{(M_i+M_f)}{2} q_i^2 \left[\frac{\Gamma_1(t)}{\frac{1}{2}(M_i+M_f)} + 2\Gamma_2(t) \right], \tag{29}$$

which implies

$$F_{++} = -\frac{3}{2} \frac{(M_i+M_f)}{2} t^{1/2} q_i z_t \left[\frac{\Gamma_1(t)}{\frac{1}{4}t} + \frac{\Gamma_2(t)}{\frac{1}{2}(M_i+M_f)} \right],$$
$$F_{+-} = -(1-z_t^2)^{1/2} \frac{3}{2} \frac{(M_i+M_f)}{2} \times q_i \left[\frac{\Gamma_1(t)}{\frac{1}{2}(M_i+M_f)} + 2\Gamma_2(t) \right]. \tag{30}$$

[7] M. Jacob and G. C. Wick, Ann. Phys. (N. Y.) **7**, 404 (1959).

[8] P. Federbush, M. Goldberger, and S. Treiman, Phys. Rev. **112**, 642 (1958).

Introducing pole fits for the form factors,

$$\Gamma_i(t)=\gamma_i/(m^2-t-i\epsilon),\quad \mathrm{Im}\Gamma_i(t)=\pi\gamma_i\delta(m^2-t),\qquad(31)$$

and applying (30) and (23), we find

$$A(t,s)=\frac{6\pi\gamma_2(s-u)}{(m^2-t)};$$
$$B(t,s)=-12\pi\left(\frac{\gamma_1}{(m^2-t)}+\frac{\gamma_2(M_i+M_f)}{(m^2-t)}\right).\qquad(32)$$

Calculations and experimental data give for $\pi\pi\to N\bar{N}$,[9]

$$\frac{\gamma_1{}^\rho}{\gamma_2{}^\rho}=\frac{G_{1\rho}(0)}{G_{2\rho}(0)}\approx\frac{0.5e}{1.83e/2M};\quad \gamma_1\approx-1.0.\qquad(33)$$

Since there is at present no experimental information on most reactions of the type we are considering, it is advantageous from the viewpoint of finding forces in meson-baryon scattering to assume the validity of $SU(3)$ and adopt a Lagrangian formulation[10] in terms of the vector and tensor couplings of vector mesons to baryons. Substituting the normalization

$$f_{\rho NN}f_{\rho\pi\pi}/4\pi=-3\gamma_1,\quad g_{\rho NN}f_{\rho\pi\pi}/4\pi=3M\gamma_2,\qquad(34)$$

into (32) and using (11) and (10a), we find the following forces for the vector and tensor coupling of vector mesons to baryons (still ignoring isospin crossing),

$$f_{l\pm}{}^V(s)=\frac{g_1{}^Vg_2}{4\pi}\frac{1}{k_ik_fW}\left\{[(E_i+M_i)(E_f+M_f)]^{1/2}\left(W-\frac{M_i+M_f}{2}\right)Q_l(y')\right.$$
$$\left.+[(E_i-M_i)(E_f-M_f)]^{1/2}\left(W+\frac{M_i+M_f}{2}\right)Q_{l\pm1}(y')\right\},\qquad(35)$$

$$f_{l\pm}{}^T(s)=\frac{g_1{}^Tg_2}{4\pi}\frac{1}{W}\{[((E_i+M_i)(E_f+M_f))^{1/2}(y'-1)+2W]Q_l(y')+[((E_i-M_i)(E_f-M_f))^{1/2}(y'+1)-2W]$$
$$\times Q_{l\pm1}(y')-[(E_i+M_i)(E_f+M_f)]^{1/2}\delta_{l0}-[(E_i-M_i)(E_f-M_f)]^{1/2}\delta_{l\pm1,0}\},\qquad(36)$$

where

$$y'=\frac{M^2+2E_iE_f-M_i{}^2-M_f{}^2}{2k_ik_f}.$$

Equations (22), (35), and (36) constitute the set of forces which we shall analyze further in the next section and apply to specific particle reactions in the final section of this paper.

4. ISOTOPIC SPIN CROSSING, UTILIZATION OF $SU(3)$, AND COMMENTS UPON THE DERIVATIONS

The first topic treated in this section is the determination of the isospin-crossing coefficients for a general two-particle meson-baryon scattering process. There are several alternative methods which may be used, and in fact, were used in the course of the research which this paper describes. We present only one of these here since it is simple, rapid, and very useful in handling multichannel scattering processes.

The group which expresses the structure of the isospin formalism, $SU(2)$, is a subgroup of $SU(3)$. A well-known conjecture[11] is that all the strongly interacting particle states belong to irreducible representations of $SU(3)$. (The actual validity of this assumption is not critical to our argument.) In particular, we assume that the two-particle meson-baryon states are linearly related to the irreducible representations, **1**, $\mathbf{8}_S$, $\mathbf{8}_A$, **10**, $\overline{\mathbf{10}}$, **27**, a relationship expressed in several sets of tables now in print.[12] For instance, the pion-nucleon state with isospin $\frac{1}{2}$ is given by

$$N\pi_{T=1/2}=-(1/\sqrt{20})(|\mathbf{27}\rangle+3|\mathbf{8}_S\rangle$$
$$+\sqrt{5}|\mathbf{8}_A\rangle+\sqrt{5}|\overline{\mathbf{10}}\rangle)\qquad(37)$$

where we have adopted a certain choice of phase between the $SU(3)$ states. Further, the crossing properties of Figs. 1(b), 1(c) have been calculated in several places,[13–15] and are reproduced in Appendix 1. We can therefore express any reaction of this type as

$$T_{fi}=\langle f|T_1\mathcal{P}_1+T_{8_S}\mathcal{P}_{8_S}+T_{8_A}\mathcal{P}_{8_A}+T_{10}\mathcal{P}_{10}$$
$$+T_{\overline{10}}\mathcal{P}_{\overline{10}}+T_{27}\mathcal{P}_{27}+T_{8_S8_A}\mathcal{P}_{8_S8_A}|i\rangle$$

where the subscripts i, f denote two-particle meson-baryon states of some definite isospin. Upon expressing the initial and final particle states in terms of $SU(3)$ states, we find the transition matrix element T_{fi} in terms of known quantities such as the $SU(3)$ crossing element, the masses of the various particles, and the coupling constants which represent each of the vertices. Before we give an example of this procedure, we mention a few words about the coupling constants. Since the

[9] J. Ball and D. Wong, Phys. Rev. **133**, B179 (1964).

[10] P. Carruthers in *Lectures in Theoretical Physics* (University of Colorado Press, Boulder, Colorado, 1964), Vol. 7, p. 82.

[11] M. Gell-Mann, Phys. Rev. **125**, 1067 (1962).

[12] P. Tarjanne, Carnegie Institute of Technology Report No. NYO-9290A (unpublished).

[13] R. E. Cutkosky, Ann. Phys. (N. Y.) **23**, 432 (1963).

[14] A. W. Martin and K. Wali, Nuovo Cimento **31**, 1324 (1964).

[15] J. DeSwart, Nuovo Cimento **31**, 420 (1964).

experimental information regarding coupling constants is quite meager, we are forced to assume the validity of $SU(3)$ values which, according to some indications,[16,17] may be poor approximations in several cases. These are taken from $SU(3)$ invariant Lagrangians which are presented in Appendix 1. We now find the isospin crossing coefficient associated with the baryon exchange contribution to the reaction $N\pi \to \Sigma K$ in the isospin one-half channel. Using the wave function,

$$\Sigma K_{T=1/2} = -(1/\sqrt{20})(|\mathbf{27}\rangle + 3|8_S\rangle - \sqrt{5}|8_A\rangle - \sqrt{5}|\overline{\mathbf{10}}\rangle)$$

along with (37), and reading off the appropriate $SU(3)$ crossing elements from the table in Appendix 1, we find

$$\langle \Sigma K|T|N\pi\rangle = (1/20)(T_{27} + 9T_{8_S} + 5T_{8_A} + 5T_{\overline{10}}),$$

$$= \frac{g_{N\pi}{}^2}{20}\left[\frac{4}{3}(1-2f+4f^2) - 18(1-2f+4f^2) + \frac{10}{3}(5-10f-4f^2) - \frac{40}{3}(1-5f+4f^2)\right],$$

$$= g_{N\pi}{}^2(2/3)(-10f^2+5f-1),$$

where all kinematical quantities have been omitted and f is the $\bar{B}BP$ vertex mixing parameter. The above crossing element is a linear combination of the Λ and Σ exchange contributions which we can find separately as follows:

$$\langle \Sigma K|T|N\pi\rangle = \alpha\langle \Sigma K,\Lambda,N\pi\rangle + \beta\langle \Sigma K,\Sigma,N\pi\rangle,$$

$$\tfrac{2}{3}g_{N\pi}{}^2(-10f^2+5f-1) = \alpha g_{\pi\Lambda\Sigma}g_{N\Lambda K} + \beta g_{\pi\Sigma\Sigma}g_{N\Sigma K},$$

$$= -\tfrac{2}{3}\alpha(1+f-2f^2) + \beta(2f-4f^2),$$

from which we find $\alpha=1$, $\beta=2$ so that the isospin crossing is $(\Sigma K,\Lambda,N\pi)+2(\Sigma K,\Sigma,N\pi)$. The method just applied is valuable in that once the phases of the coefficients connecting the $SU(3)$ and particle bases have been fixed, the phase convention for any meson-baryon single-particle-exchange reaction is known. We present a list of the relevant wave functions and crossing coefficients in Appendix 1.

The expression for forces generated in the s channel by processes in the u channel, Eq. (22), was left in terms of decay widths Γ_i. In some cases, it is preferable to express the forces in terms of $SU(3)$ coupling constants, so we now find how to relate widths to coupling constants using much the same technique as exhibited in the previous section. For purposes of clarity, we specialize to a particle of angular momentum, $j=1+$, giving other relevant results in Appendix 1. We start by defining amplitudes $A^s(s,t)$, $B^s(s,t)$ as

$$\begin{pmatrix} A^s(s,t) \\ B^s(s,t) \end{pmatrix} = \frac{1}{\pi}\int^{\infty} \frac{ds'}{(s'-s)}\,\mathrm{Im}\begin{pmatrix} A(s',t) \\ B(s',t) \end{pmatrix}, \tag{38}$$

where the lower limit of integration covers all bound states in the s channel, and we temporarily ignore isospin. Applying (6) in the case of elastic scattering, we find

$$\begin{pmatrix} f_1 \\ f_2 \end{pmatrix} = \frac{1}{\pi}\int \frac{ds'}{s'-s}\mathbf{C}(s,s')\,\mathrm{Im}\begin{pmatrix} f_1 \\ f_2 \end{pmatrix},$$

$$\mathbf{C}(s,s') = \boldsymbol{\alpha}^{-1}(s)\boldsymbol{\alpha}(s') = \frac{1}{2W}\begin{pmatrix} \dfrac{(W+\sqrt{s'})(E+M)}{E'+M} & \dfrac{(W-\sqrt{s'})(E+M)}{E'-M} \\ \dfrac{(\sqrt{s'}-W)(E-M)}{E'+M} & \dfrac{(W+\sqrt{s'})(E-M)}{E'-M} \end{pmatrix}. \tag{39}$$

From (5a), we have

$$f_1 = 3xf_{1+}, \quad f_2 = -f_{1+},$$

also assuming the resonance approximation,

$$\mathrm{Im}f_{1+}(s') = \frac{\pi\Gamma(s)}{k(s)}\delta(s'-M^2)W_r.$$

Integrating, and including the isotopic weight of the particle in the direct channel α, we find

$$f_{1+}(s) = C_{11}(s,M^2)\frac{\Gamma(s)}{k(s)}W_r\frac{\alpha}{M^2-s}.$$

If we assume the width for a particle of spin $j=l\pm$ has the energy dependence

$$\Gamma(s) = \Gamma_r\left(\frac{k}{k_r}\right)^{2l+1}, \tag{40}$$

then

$$f_{1+}(s) = \frac{\alpha W_r{}^2}{(W_r+M)^2-m^2}\frac{k^2}{k_r{}^3}\frac{\Gamma_r}{2} \times \frac{(W+M)^2-m^2}{W^2}\frac{1}{M-W}. \tag{41}$$

From (41), we define the coupling constant as

$$g^2 = \frac{\alpha}{2k_r{}^3}\frac{\Gamma_r W_r{}^2}{(W_r+M)^2-m^2}. \tag{42}$$

[16] K. Wali and R. Warnock, Phys. Rev. **135**, B1358 (1964).
[17] V. Gupta and V. Singh, Phys. Rev. **136**, B782 (1964).

The connection with $SU(3)$ is seen by treating the $N^*N\pi$ vertex as an example. The $SU(3)$-invariant Lagrangian reads, omitting space-time dependence,

$$\mathcal{L}=g_D^2(\sqrt{2}\bar{N}^*N\pi+\cdots),$$

and so, in order to find the over-all coupling g_0^2 from experiment, we note $g_0^2=0.5g_{N^*N\pi}$ which gives $g_0^2=0.22(\mu^{-2})$.

The final part of this section is devoted to a study of some features of the forces we derived in the previous section. We first consider the limiting values of Eqs. (22), (35), and (36) for asymptotically large values of the center-of-mass energy W. The results are

u-channel exchange [Eq. (22)] of a particle with $j=l'\pm\frac{1}{2}$:

$$f_{l\pm}\sim W^{2(l'-1)\pm1}\ln W,\text{ which diverges for}$$

$$l'\geqslant\begin{pmatrix}1\\2\end{pmatrix}\quad\text{if}\quad J=\begin{pmatrix}l'+\frac{1}{2}\\l'-\frac{1}{2}\end{pmatrix};\tag{43}$$

t-channel exchange of a vector meson [Eqs. (35) and (36)]:

$$f_{l\pm}\sim\ln W,\text{ which diverges.}\tag{44}$$

This is the well-known divergence of forces arising from the exchange of high-spin objects. The result is undoubtedly unphysical and means that the concept which we assumed of a "particle" as a structureless entity is incorrect. The application of Regge poles offers at present a promising approach to this problem but the theory is still rather inchoate. At low energies, we hopefully expect that our forces differ in an insignificant way from the Regge pole forces. For instance, consider the force generated in πN scattering by nucleon exchange. The work of Frautschi and Walecka[3] indicates that the physics in the low-energy tail of the πN physical region is dominated by the near or "static" exchanged nucleon cut. Any point on this cut corresponds to a range of values of u, the largest such range being $M^2-2m^2<u<M^2+2m^2$. Estimating the slope of the nucleon trajectory from the $N(938)$ and $N^{***}(1688)$ masses, and applying a straight line approximation over this range of u, we find that the nucleon's angular momentum changes by about 4% and so our assumption of fixed angular momentum is a good one in this case. Unfortunately, the situation is worse for the exchange of high-spin objects since a large contribution to the low-energy force comes from the far left-hand cut $0>s$, in some cases.[18] Since the Legendre expansion (5a) diverges for almost all the region $s<0$, we are in doubt about the predicted forces we find for the exchange of continuum states. That is, in situations where the "static" pole is not large, all we can hope is that for low energies, the Regge amplitude is approximated to some degree by a truncated Legendre expansion.

[18] E. Golowich (unpublished).

Early in the derivations last section, we decided on fixed s instead of, say, fixed t dispersion relations. In an approximation scheme where one does not evaluate the single dispersion integrals exactly, different results are, in general, found depending upon which is used. Let us now consider the u-channel contribution, (12), where we eventually make the sharp resonance approximation in calculating forces generated by u-channel poles. Our approach is to continue the pole terms from the physical u channel to the physical s channel by fixing the cosine of the angle of scattering,

$$x_u=(t+2E_i^uE_f^u-M_i^2-M_f^2)/2k_i^uk_f^u$$

as follows. We use the Mandelstam relation,

$$t=M_i^2+M_f^2+m_i^2+m_f^2-s-u$$

and evaluate all quantities in the cosine which depend upon u at the pole position, $u=M_r^2$. If, instead, one evaluates the u-dependent quantities at $u=M_r^2$, but fixes the momentum transfer t,

$$t=-2k_ik_f\left(\frac{(2E_iE_f-M_i^2-M_f^2}{2k_ik_f}-x\right),$$

then one finds that, if the orbital angular momentum of the exchanged state l' is less than or equal to the orbital angular momentum of the direct channel l, the forces are identical. Otherwise, this is not the case.[19]

5. APPLICATIONS

We shall now analyze low-energy meson-baryon reactions in terms of the long-range forces which have been derived. The maximum momentum transfer for such reactions at a given center-of-mass energy W is twice the center-of-mass momentum $2k$, and for small enough k, say, $k<M+m=$ baryon mass+meson mass, we expect the long-range effects to dominate. Our forces are real, and constitute an approximation to the "Born phase shift",

$$f_{l\pm}(W)q_i^{1/2}q_f^{1/2}=e^{i\delta_{l\pm}}\sin\delta_{l\pm}\approx\delta_{l\pm}\quad\text{if}\quad\delta_{l\pm}<1.\tag{45}$$

Using a CDC-1604 computer, we calculated the approximate Born phase shifts for the partial waves 0+ to 5− in all two particle channels at ten energies in the low-energy region. The forces are generated by the exchange of the following $SU(3)$ multiplets (the letters B, D, etc., indicate the notation we use in tables which appear later).

1. Baryon (mixing parameter=0.35) (B).
2. Decuplet (D).
3. Vector meson.
   (a) Vector coupling (mixing parameter=1.0) (V_V).
   (b) Tensor coupling (mixing parameter=0.25) (V_T).
4. $Y_0^*(1520)$ singlet (S).
5. $D_{3/2}$ octet (mixing parameter=0.40) (O).

[19] B. Thomas, Cornell University, 1964 (unpublished).

We choose to exchange only those multiplets which have been confirmed experimentally. Further experimental evidence may allow us to expand this program with the addition of an octet of $j=3-$ resonances and a decuplet of $j=3+$ resonances. Of the former, only $N^*(1688)$ and $Y_0^*(1815)$ have been found while for the latter $N^*(1920)$ is the only confirmed state. Actual masses are used to describe all particles, and $SU(3)$ estimates for coupling constants, normalized to the experimentally determined value as in the previous section, are adopted. For a definite strangeness and isospin state, the output for a given energy generally consists of a matrix since several two-particle meson baryon states can have the same quantum numbers. We also find the diagonal form of such a matrix since this gives us information regarding $SU(3)$ amplitudes.[20]

(a) S-Wave $N\pi$, NK, $N\bar{K}$ Reactions

As a first attempt to check the consistency of our forces with low-energy phenomena, we examine the S-wave Born phase shifts for πN, KN, $\bar{K}N$ reactions. Ross[21] has performed an analysis of these using the inverse matrix amplitude technique and found the results to be consistent with the exchange of an octet of vector mesons with pure F coupling. Our results are shown in Fig. 2. In all but the $S=-1$, $T=0$, 1 channels, the vector meson exchange with vector coupling is dominated by other forces, which seems to contradict Ross' result. However, Table I, which relates the total

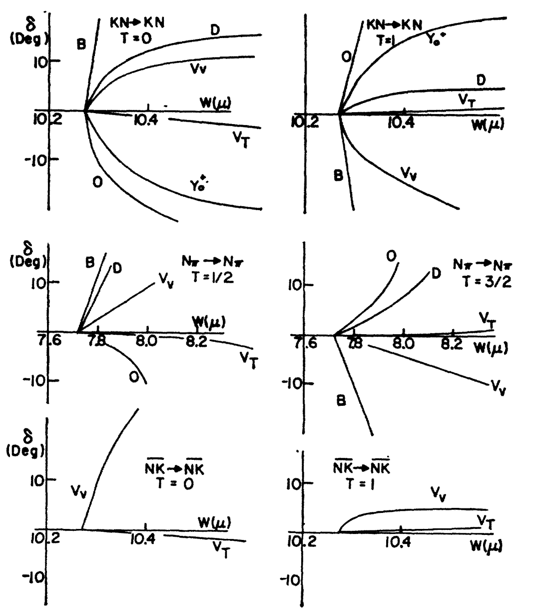

FIG. 2. S-wave Born phase shifts δ (deg) as a function of center-of-mass energy W in pion masses μ. The reactions considered are $T=0$, 1 KN; $T=\frac{1}{2}$, $\frac{3}{2}$ πN; $T=0$, 1 $\bar{K}N$ elastic scattering.

[20] A. W. Martin and K. Wali, Phys. Rev. **130**, 2455 (1963).

[21] M. Ross, Bull. Am. Phys. Soc. **9**, 629 (1964).

TABLE I. S-wave Born phase shifts (deg). (Center-of-mass energy W in pion masses μ.)

Channel	$S=1$, $T=0$	$S=1$, $T=1$	$S=-1$, $T=0$	$S=-1$, $T=0$	$S=0$, $T=\frac{1}{2}$	$S=0$, $T=\frac{3}{2}$
W (μ)	10.3	10.3	10.3	10.5	7.8	7.8
δ_{total}	8.5	−11.6	8.5	5.6	17.0	−6.0
δ_{VV}	3.5	−7.0	9.0	5.0	3.0	−1.5

Born phase shift to that of vector meson exchange, is rather interesting. In all cases, the two have the same sign, and except for $S=0$, $T=\frac{1}{2}$, the magnitudes are not too far apart. If our forces do represent reality to some degree, then the low-energy physics seems to be more complicated than an analysis of scattering lengths would indicate. Of course, our forces could be incorrect and, for instance, the fixed t description could be valid. However, again it is found that, e.g., in the channels $S=0$, $T=\frac{1}{2}$, $\frac{3}{2}$, the nucleon exchange term is far larger than the vector-meson contribution. Therefore, all we can say is that our description seems consistent with experimental S-wave data, although it is certainly not clear that various short-range forces which we have ignored are insignificant (witness the suspiciously large contribution from the $D_{3/2}$ states).

(b) Low-Energy Resonances

Our primary aim in studying meson-baryon forces is to reproduce the low-energy structure. The most convenient way to classify the large set of numbers which we have calculated is according to $SU(3)$ multiplets, and possible Regge recurrences. Because we do not consider either short-range forces or the contribution of the unitarity integral over the right-hand cut, it is not possible for us to determine the wave function (and hence branching ratios) of any resonance discovered in this analysis. Rather, the association with $SU(3)$ states allows us to relate the classified bound states and resonances generated in various isospin and hypercharge channels. Although the symmetry is badly broken for long-range forces at low energies, it is still possible to apply the concept of $SU(3)$ to diagonalized Born-phase-shift matrices. We can identify the various irreducible representations of $SU(3)$ by examining the eigenvectors of the diagonalized matrix since we know the relation between the particle and $SU(3)$ bases from our isospin-crossing technique. As an example of this we consider diagonalization of the Born-phase-shift matrix with quantum numbers $S=0$, $T=\frac{1}{2}$, $j=3-$ generated by baryon-exchange forces at energies $W=13$, 14.5 pion masses in the center-of-mass system. The relevant eigenvector amplitudes are given in Table II. Since we use real masses in our calculation, the eigenvectors found from diagonalizing the force matrix do not equal the $SU(3)$ eigenvector, but tend towards it as the energy is increased and mass-breaking effects become less significant. However, even in the example shown in

TABLE II. Eigenvectors of Born-phase-shift matrix (deg) for channel $S=0$, $T=\frac{1}{2}$.

		SU(3) prediction			
	Particle component	8	8′	10	27
	$N\pi$	−0.67	−0.5	−0.5	−0.67
	ΛK	−0.22	−0.5	0.5	0.67
	ΣK	−0.67	+0.5	+0.5	−0.22
	$N\eta$	−0.22	0.5	−0.5	0.22

	Actual eigenvectors							
	$W=13.0\,\mu$				$W=17.0\,\mu$			
Particle component	8	8′	10	27	8	8′	10	27
$N\pi$	−0.97	−0.04	−0.07	−0.22	−0.95	−0.14	−0.08	−0.26
ΛK	−0.01	−0.22	0.89	0.39	−0.02	−0.36	0.79	0.49
ΣK	−0.02	+0.97	+0.24	−0.0	−0.09	+0.88	+0.43	−0.03
$N\eta$	−0.2	0.08	−0.37	0.90	−0.3	0.21	−0.43	0.82

Table II, one of the largest cases of mass breaking we treated, the association can be made. In case the exchange of a multiplet, e.g., D, V_T, leads to the transitions, $\mathbf{8}\leftrightarrow\mathbf{8}'$, in the direct channel, we modify the above prescription somewhat. The appropriate $SU(3)$ eigenvectors are not $\mathbf{8}$, $\mathbf{8}'$, but rather $\mathbf{8}^{(1)}$, $\mathbf{8}^{(2)}$, the linear combination of $\mathbf{8}$, $\mathbf{8}'$ determined by diagonalizing that 2×2 submatrix of the $SU(3)$ crossing matrix which describes the transitions $\mathbf{8}\to\mathbf{8}$, $\mathbf{8}'\to\mathbf{8}'$, $\mathbf{8}\to\mathbf{8}'$.

(*i*) *Decuplet Trajectory*

It has been conjectured that there is an intimate dynamical relationship between the $j=1+$ and $j=3+$ baryonic resonances.[22] In Figs. 3 and 4, we plot the diagonalized phase shifts for $j=1+$ and $j=3+$, respectively in the states $S=0$, $T=\frac{3}{2}$; $S=-1$, $T=1$; $S=-2$, $T=\frac{1}{2}$, and $S=-3$, $T=0$. The most significant future of each angular momentum state is the large amplitude for $\mathbf{10}$. There are attractions for $\mathbf{27}$ and $\mathbf{8}^{(1)}$ but these are down by at least a factor of three. The resonances N*(1238), Y_1*(1385), Ξ*(1520), and Ω⁻(1676)

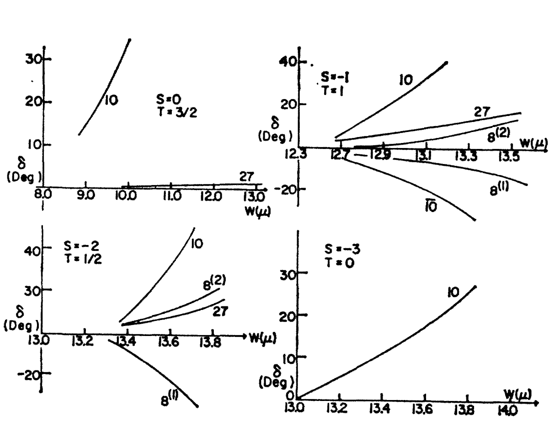

FIG. 3. $j=1+$ Born eigenphase shifts δ (deg) as a function of W (μ) in the channels $S=0$, $T=\frac{3}{2}$; $S=-1$, $T=1$; $S=-2$, $T=\frac{1}{2}$; $S=-3$, $T=0$.

[22] P. Carruthers, Phys. Rev. Letters **12**, 259 (1964).

verify our findings for the $j=1+$ state, but at present only one of the $j=3+$ states, N***(1920), has been detected experimentally. Our results indicate that relatively large attractions occur for $j=3+$ in the channels ($S=-1$, $T=1$), ($S=-2$, $T=\frac{1}{2}$), and ($S=-3$, $T=0$), with($S=2$, $T=\frac{1}{2}$) especially favorable. The dynamics of these large phase shifts is shown in Table III in which we

TABLE III. Born phase shifts ($j=1+$, $3+$) in channels $S=0$, $T=\frac{3}{2}$, and $S=-3$, $T=0$.

	δ (deg)					
	$S=0$, $T=\frac{3}{2}$				$S=-3$, $T=0$	
Exchanged states	$j=1+$ $W=13\,\mu$ 10	27	$j=3+$ $W=13\,\mu$ 10	27	$j=1+$ $W=14\,\mu$	$j=3+$ $W=16\,\mu$ 10
B	83.2	5.8	5.4	0.02	19.8	2.3
D	−2.6	−0.4	−0.06	0.0	−2.3	−0.14
V_V	−12.5	−1.6	−0.02	−0.87	2.9	0.85
V_T	39.0	3.4	2.89	0.03	10.0	2.5
S	3.5	−3.5	0.02	−0.02	6.3	0.60
O	−40.0	−2.6	0.6	0.0	−4.6	−0.30
Total	70.6	1.1	7.6	−0.9	32.1	5.5

list the various exchange contributions to $j=1+,3+$ at a given energy for the channels ($S=0$, $T=\frac{3}{2}$) and ($S=-3$, $T=0$). In each channel, it is the baryon and vector meson (tensor coupling) exchange which provide the main attrac-

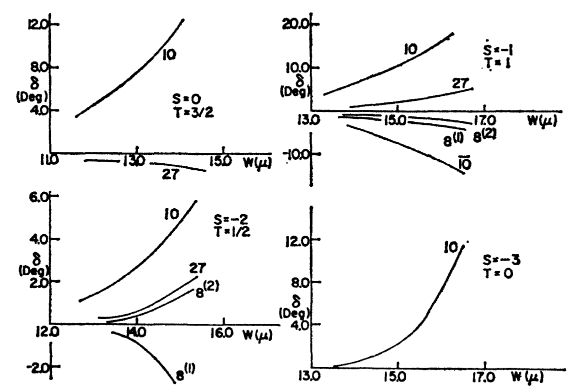

FIG. 4. $j=3+$ Born eigenphase shifts, δ (deg), as a function of W (μ) in the channels $S=0$, $T=\frac{3}{2}$; $S=-1$, $T=1$; $S=-2$, $T=\frac{1}{2}$; $S=-3$, $T=0$.

TABLE IV. Born phase shifts ($j=3-$) in channels ($S=0$, $T=\frac{1}{2}$), ($S=-1$, $T=0$), ($S=-1$, $T=1$), and ($S=-2$, $T=\frac{1}{2}$).

S	T	W	$SU(3)$ state	δ (deg) exchanged state B	D	V_V	V_T	S	O	Total
0	$\frac{1}{2}$	14μ	$8^{(1)}$	0.96	8.90	5.40	12.5	0.00	−0.2	27.7
			$8^{(2)}$	0.01	−0.3	1.15	−0.6	−0.01	0.00	0.04
			$\overline{10}$	0.06	0.31	0.30	2.20	−0.01	−0.01	2.85
			27	−0.19	0.11	−0.9	−0.99	0.01	0.02	−1.93
−1	0	16μ	$8^{(1)}$	1.1	17.3	8.12	16.9	0.10	−0.03	43.6
			$8^{(2)}$	0.03	−0.98	2.92	−3.14	−0.04	0.00	−2.11
			10	−0.39	−19.8	14.0	8.1	0.06	0.13	2.05
			27	−0.66	0.46	−2.2	−1.7	0.04	0.00	−4.1
−1	1	16μ	$8^{(1)}$	1.90	9.50	3.46	14.4	0.05	−0.3	28.7
			$8^{(2)}$	0110	−7.3	7.11	−6.34	−0.10	−0.02	−6.5
			10	−2.0	3.6	−0.5	−9.5	−0.04	0.5	−7.9
			$\overline{10}$	0.30	0.28	0.02	4.40	−0.05	−0.05	4.9
			27	−0.2	1.35	−3.7	−1.75	0.04	0.06	−4.3
−2	$\frac{1}{2}$	15μ	$8^{(1)}$	0.3	3.0	3.03	3.83	0.02	−0.03	6.42
			$8^{(2)}$	0.05	−1.3	2.10	−2.80	0.0	0.01	−1.3
			10	−0.9	0.88	0.17	−3.93	−0.02	0.10	−2.8
			27	−0.1	0.05	−0.73	0.39	0.0	0.03	−0.3

tion, and $D_{3/2}$ octet exchange the main repulsion. However, the relative importance of the baryon- and vector-exchange terms is different in the $S=0$ and $S=-3$ channels. This shows that the actual long-range forces may have values far removed from the $SU(3)$ estimates.

(ii) *Baryon Trajectory*

The $j=1-$, $3-$ states receive large attractive forces from the exchange of the $j=1+$ states. Therefore, at our level of calculation, Chew's "reciprocal bootstrap" mechanism[23] extends to the $SU(3)$ case. The results are given in Table IV and Fig. 5. In all the $j=3-$ states, the combined effect of the vector-meson exchange terms is greater than that of decuplet exchange, while in the $j=1-$ state, they are roughly equal. This implies that any realistic "bootstrap" calculation attempting to generate the meson-baryon spectrum should include the exchange forces of the vector mesons.

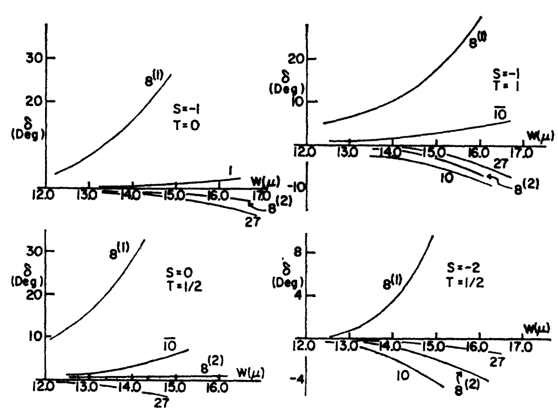

FIG. 5. $j=3-$ Born eigenphase shifts, δ (deg), as a function of W (μ) in the channels $S=0$, $T=\frac{1}{2}$; $S=-1$, $T=0$, 1; $S=-2$, $T=\frac{1}{2}$.

[23] G. Chew, Phys. Rev. Letters 9, 233 (1962).

The only $j=3-$ states found experimentally so far are the resonances in the ($S=0$, $T=\frac{1}{2}$) and ($S=-1$, $T=0$) channels. As seen in Table IV, the forces in the remaining channels of the predicted octet are rather small compared to those of the occupied channels, and inelastic effects may be playing a dominant role.

(iii) *$Y_0^*(1520)$ Unitary Singlet*

The only remaining angular momentum and $SU(3)$ channel having attractive forces so large and rapidly varying that a resonance or bound state is clearly predicted is the $D_{3/2}$ ($S=-1$, $T=0$) unitary singlet state. Figure 6 shows the forces which contribute to the unitary singlet, and Fig. 7 exhibits the domination of the unitary-singlet phase shift over the phase shifts of $8^{(1)}$, $8^{(2)}$, and **27**. The largest attractive force comes from decuplet exchange, and the sum of the vector-meson exchange forces is also significant. An examination of the remaining angular momentum states indicates that it is unlikely that any other unitary singlet states are generated by elastic forces, except possibly in the S state.

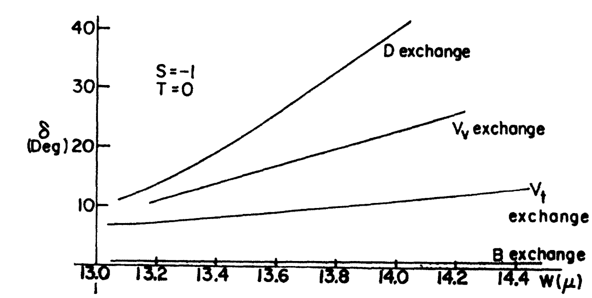

FIG. 6. $j=2-$ Born phase shift, δ (deg), contributions of baryon, $j=1+$ decuplet, vector meson (vector and tensor coupling) exchange forces in the singlet $SU(3)$ state as a function of W (μ).

TABLE V. Born phase shifts ($j=2+$) in channels ($S=0$, $T=\frac{1}{2}$); ($S=-1$, $T=0$), ($S=-1$, $T=1$), and ($S=-2$, $T=\frac{1}{2}$).

S	T	W	$SU(3)$ state	B	D	V_V	V_T	S	O	Total
				δ (deg) exchanged state						
0	$\frac{1}{2}$	14μ	$\mathbf{8}^{(1)}$	17.5	1.13	3.20	−30.3	0.79	−4.9	−12.6
			$\mathbf{8}^{(2)}$	2.55	0.24	9.30	2.62	−0.79	−0.03	9.0
			$\overline{\mathbf{10}}$	0.80	−0.04	0.73	−6.2	−0.7	−0.71	−6.1
			27	−5.50	−0.44	−2.30	2.04	0.7	1.40	−4.1
−1	0	16μ	$\mathbf{8}^{(1)}$	17.0	1.22	13.7	−39.1	2.00	−1.60	−4.8
			$\mathbf{8}^{(2)}$	1.0	0.40	6.80	7.60	−2.00	−2.70	11.1
			1	−7.0	−2.6	24.0	−18.0	3.20	5.30	4.9
			27	−10.0	−0.6	−4.7	4.20	2.10	1.80	7.9
−1	1	16μ	$\mathbf{8}^{(1)}$	20.0	2.23	6.7	−37.8	2.45	−10.0	−11.3
			$\mathbf{8}^{(2)}$	3.0	−0.50	12.4	14.7	−3.0	−1.9	25.2
			10	−40.7	0.7	−1.0	21.7	2.5	14.8	−2.1
			$\overline{\mathbf{10}}$	7.2	−0.1	0.03	−11.5	−2.0	−2.4	10.8
			27	−6.6	0.24	−6.8	4.5	2.0	3.6	−3.1
−2	$\frac{1}{2}$	15μ	$\mathbf{8}^{(1)}$	7.2	2.6	5.03	−9.9	4.6	−2.1	7.4
			$\mathbf{8}^{(2)}$	1.3	−1.21	6.70	7.4	−2.5	−0.1	11.7
			10	−17.0	0.73	0.49	10.0	−4.6	3.9	−6.5
			27	−3.0	0.11	−2.0	−1.2	2.5	1.2	−2.4

(c) Other Channels

In Part (b) of this section we studied channels for which our dynamical mechanism provides an explanation of experimentally determined bound states and resonances. We now consider situations in which an experimentally produced resonance may not be explainable mainly in terms of elastic forces.

The dynamics of the $D_{3/2}$ octet has been analyzed[24] in the framework of the Cook-Lee model,[25] which uses an inelastic mechanism. Our study of the $D_{3/2}$ states yields results shown in Figs. 7 and 8. There are attractions for both octet states, but they are rather small and slowly varying compared to the phase shifts we found in the preceding part, so it is difficult to believe that the observed resonances could depend to any large degree upon elastic forces.

We next turn to $Y_1^*(1765)$ which lies in the $j=2+$ angular momentum channel. The Born-phase-shift plot in Fig. 9 implies that if this resonance is the result of elastic forces, then it must belong to an $SU(3)$ multiplet $\mathbf{8}^{(2)}$. We list the Born phase shifts at a given energy for the states of the full octet in Table V. The most attractive forces do lie in $\mathbf{8}^{(2)}$, but are seemingly not sufficient to produce an octet of resonances. In particular, mass breaking effects so vitiate the ($S=0$, $T=\frac{1}{2}$) channel phase shift that it seems unlikely a resonance will occur there. Hence, a study of the long-range forces in this case implies that one or more members of a given multiplet may not be experimentally observable as a resonance.

Our next application is an examination of the representation **27** in two channels, ($S=-1$, $T=2$) and ($S=-3$, $T=1$). This multiplet has been the object of many speculations, both experimental and theoretical.[26] In Tables VI and VII we present the Born phase shifts for all partial waves up to $j=5\pm$. The only signs of structure, aside from the somewhat unreliable S-wave phase

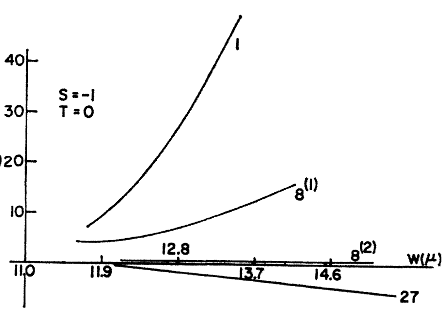

FIG. 7. $j=2-$ Born eigenphase shifts, δ (deg), as a function of $W(\mu)$, in the channel $S=-1$, $T=0$.

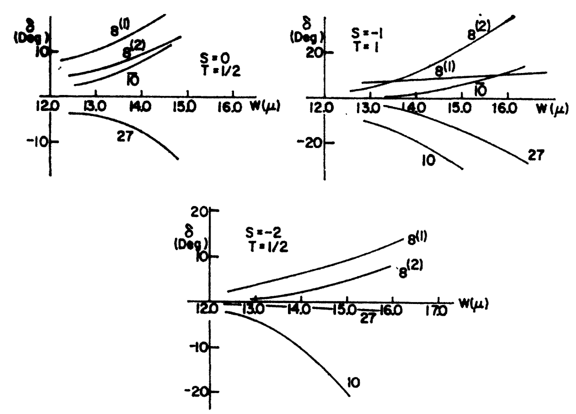

FIG. 8. $j=2-$ Born eigenphase shifts, δ (deg), as a function of $W(\mu)$ in the channels $S=0$, $T=\frac{1}{2}$; $S=-1$, $T=1$; $S=-2$, $T=\frac{1}{2}$.

[24] J. Brehm, Phys. Rev. **136**, B216 (1964).
[25] L. Cook and B. Lee, Phys. Rev. **127**, 283 (1962).

[26] For instance, we cite: R. Alvarez *et al.*, Phys. Rev. Letters **12**, 710 (1964); D. Kleitman and S. Glashow, Phys. Letters **11**, 84 (1964); Y. Pan and R. P. Ely, Phys. Rev. Letters **13**, 277 (1964); B. Diu and H. R. Rubinstein, CERN, 1965 (unpublished).

TABLE VI. Born phase shifts ($j=0+$ to $5-$) in channel $S=-1$, $T=2$.

	δ (deg)					
$W(\mu)$	10	14	14	17	17	
$j=l\pm$	0+	1+	1−	2+	2−	
B	−49.0	29.0	−15.1	−13.6	3.8	
D	6.8	−2.07	19.2	0.11	−9.5	
V_V	−13.5	−19.4	−39.2	−14.0	−24.1	
V_T	0.2	16.3	−39.8	12.1	−16.9	
S	13.5	−16.8	8.5	10.1	−2.61	
O	24.2	−14.6	8.3	8.8	−2.1	
Total	−12.8	−9.6	−58.1	3.5	−51.4	
$W(\mu)$	17	17	17	17	17	17
$j=l\pm$	3+	3−	4+	4−	5+	5−
B	4.0	−0.73	−1.3	0.16	0.39	−0.05
D	−0.02	2.02	0.0	−0.46	0.0	0.11
V_V	−5.25	−8.74	−2.04	−3.33	−0.81	−1.31
V_T	4.5	−5.5	1.72	−1.98	0.68	−0.75
S	−2.0	0.28	0.41	−0.05	−0.08	0.01
O	−1.5	0.20	0.28	−0.03	−0.05	0.0
Total	−0.27	−12.3	−0.93	−5.70	0.13	−2.0

TABLE VII. Born phase shifts ($j=0+$ to $5-$) in channel $S=-3$, $T=1$.

	δ (deg)					
$W(\mu)$	13.1	14.5	14.5	18.0	18.0	
$j=l\pm$	0+	1+	1−	2+	2−	
B	−36.3	12.1	−5.72	−10.4	2.7	
D	5.8	−1.2	6.74	0.34	−7.4	
V_V	−15.3	−5.6	−11.8	−6.9	−12.5	
V_T	0.24	9.4	−27.4	12.92	−21.3	
S	9.71	−2.73	1.78	3.94	−1.21	
O	50.2	−10.8	5.9	13.4	−3.7	
Total	14.4	1.17	−30.5	13.3	−34.4	
$W(\mu)$	18.0	18.0	18.0	18.0	18.0	18.0
$j=l\pm$	3+	3−	4+	4−	5+	5−
B	2.76	−0.42	−0.75	0.10	0.18	−0.02
D	−0.07	1.44	0.02	−0.30	−0.00	0.07
V_V	−2.12	−3.65	−0.69	−1.15	−0.25	−0.39
V_T	3.83	−5.6	1.1	−1.65	0.40	−0.51
S	−0.72	0.16	0.14	−0.02	−0.03	0.00
O	−2.15	0.30	0.35	−0.05	−0.06	0.01
Total	1.53	−7.77	0.17	−3.1	0.24	0.52

shift, come from the $j=2+$ ($S=-3$, $T=1$) phase shift, which may even be large enough to produce a resonance, although a more sophisticated calculation including inelastic channels is needed to ascertain this. Of particular interest[26] is the $j=1+$, $S=0$, $T=\frac{1}{2}$ channel where the phase shift for **27** is small for the low-energy region due to a rather large cancellation between the strongly attractive baryon exchange force and the repulsive vector-meson (tensor-coupling) and $D_{3/2}$ singlet and octet exchange forces.

(d) Symmetry Breaking

The mass splittings among the groups of particles we have been treating as $SU(3)$ multiplets are rather

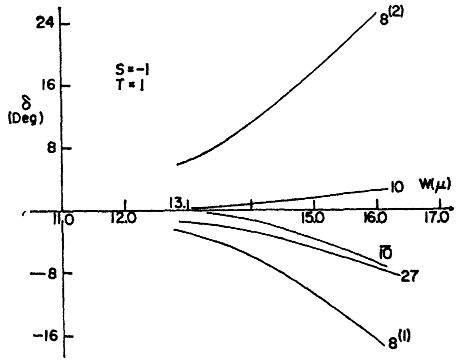

FIG. 9. $j=2+$ Born eigenphase shifts, δ (deg), as a function of $W(\mu)$ in the channel $S=-1$, $T=1$.

large[27] and imply that we should study the validity of our assumption regarding the consistency of an approximate $SU(3)$-invariant and crossing-symmetric model. That is, if one starts with an exact $SU(3)$ model and introduces mass splittings, for instance through a "spontaneous breaking" mechanism,[28] to what extent will the ordering of the single-particle-exchange forces mirror the experimental findings? There are two types of ordering to which we refer—both the relative size of the forces which generate states within a given $SU(3)$ multiplet and also the various multiplets themselves. With regard to the first type, we studied the Born terms for the individual states which make up the $j=1+$, $1-$, $3+$, $3-$ multiplets and found in all cases that the attractions in the potentially resonant states are monotonically ordered according to hypercharge, the most attractive lying in the states of largest hypercharge. This is of course in agreement with experiment, in cases where the resonant states have actually been found. Further, as seen in the typical values given in Table VIII, the equal-spacing rule holds roughly for the $j=1+$,

TABLE VIII. Symmetry-breaking effects upon long-range forces. Intramultiplet Born phase shifts.

	State	$W(\mu)$	δ(deg)	$W(\mu)$	δ(deg)
Decuplet, $j=1+$	$N^*(1238)$	13.0	70.9	···	···
	$Y_1^*(1385)$	13.0	45.8	···	···
	$\Xi^*(1530)$	13.0	18.2	···	···
	$\Omega^-(1676)$	13.0	1.24	···	···
Octet, $j=3-$	$N'(1688)$	14.0	27.0	15.0	44.0
	$Y_0{}^1(1815)$	14.0	14.0	15.0	27.0
	$Y_1'(?)$	14.0	11.0	15.0	20.0
	$\Xi'(?)$	14.0	2.0	15.0	6.0
Decuplet, $j=3+$	$N''(1920)$	15.0	14.0	16.0	22.4
	$Y_1''(?)$	15.0	10.7	16.0	18.2
	$\Xi''(?)$	15.0	6.9	16.0	12.2
	$\Omega''(?)$	15.0	2.9	16.0	7.5

[27] G. Rajasekaran, Ph.D. thesis, University of Chicago, 1964 (unpublished), investigates the extent to which the $SU(3)$ wave functions are valid for several meson-baryon resonances.

[28] R. E. Cutkosky and P. Tarjanne, Phys. Rev. **132**, 1354 (1963).

$3+$ forces whereas the Λ, Σ $j=3-$ excited states lie close together. We give no numerical values for the $j=1-$ states since at energies where all particle channels are open, the Born phase shifts are already beyond the $\delta<1$ bound of validity for the approximation, $e^{i\delta}\sin\delta\approx\delta$. Taking the average of the Born phase shifts for the states composing a given multiplet, we compared the strengths of the forces generating the intermultiplet structure. The results show, in order of decreasing attraction: $j=1-$ baryon octet, $j=1+$ decuplet, $Y_0^*(1520)$ singlet, $j=3-$ octet, $Y_1^*(1765)$ decuplet. Again a comparison of this with experiment, where possible, indicates agreement.

ACKNOWLEDGMENTS

The author expresses his thanks to Dr. Peter A. Carruthers, Bruce R. Thomas, and Dr. Frank von Hippel for stimulating conversations. The programming for the numerical calculations performed on a CDC 1604 electronic computer was done by Mrs. Joan R. Golowich.

APPENDIX I

Having utilized several features of $SU(3)$ symmetry in the course of our discussion of long-range forces in meson-baryon scattering, we present relevant details in this Appendix.

Consider the elastic scattering of the pseudoscalar-meson octet from the baryon octet. The crossing elements resulting from the exchange of various $SU(3)$ multiplets are listed in Table IX. All elements are expressed in terms of coupling constants which describe various vertices made up of three interacting $SU(3)$ multiplets. We use the Lagrangian formulation, omitting space-time dependence, to express these couplings in terms of particle states.

TABLE IX. Crossing elements resulting from the exchange of various $SU(3)$ multiplets.

Direct channel representation	Uncrossed baryon	Crossed baryon	Crossed decuplet	Crossed singlet	Crossed vector meson
1	0	$\frac{4}{3}(5-10f-4f^2)g_{N\pi}^2$	$-5g_D^2$	g_S^2	$3f_V g_{\pi N} g_{\rho\pi}$
10	0	$(8/3)(1+f-2f^2)g_{N\pi}^2$	g_D^2	$-g_S^2$	$-(1-f_V)g_{\pi N}g_{\rho\pi}$
$\overline{\mathbf{10}}$	0	$(8/3)(1-5f+4f^2)g_{N\pi}^2$	g_D^2	$-g_S^2$	$(1-f_V)g_{\pi N}g_{\rho\pi}$
27	0	$\frac{4}{3}(1-2f+4f^2)g_{N\pi}^2$	$\frac{1}{3}g_D^2$	g_S^2	$-f_V g_{\pi N}g_{\rho\pi}$
8-8	$(20/3)(1-f)^2g_{N\pi}^2$	$-2(1-2f+4f^2)g_{N\pi}^2$	$2g_D^2$	g_S^2	$\frac{3}{2}f_V g_{\pi N}g_{\rho\pi}$
8′-8′	$12f^2g_{N\pi}^2$	$-\frac{2}{3}(5-10f-4f)g_{N\pi}^2$	0	$-g_S^2$	$\frac{3}{2}f_V g_{\pi N}g_{\rho\pi}$
8-8′	$(4\sqrt{5})(1-f)fg_{N\pi}^2$	0	$+(\sqrt{5})g_D^2$	0	$(\frac{1}{2}\sqrt{5})(1-f_V)g_{\pi N}g_{\rho\pi}$
8′-8	$(4\sqrt{5})(1-f)fg_{N\pi}^2$	0	$+(\sqrt{5})g_D^2$	0	$(\frac{1}{2}\sqrt{5})(1-f_V)g_{\pi N}g_{\rho\pi}$

(a) Pseudoscalar-Meson–Baryon–Antibaryon Vertex

$$\mathfrak{L}^{BBP}=g_{N\pi}\bar{N}\boldsymbol{\tau}N\cdot\boldsymbol{\pi}+g_{\Lambda\pi}(\boldsymbol{\pi}\cdot\bar{\Lambda}\boldsymbol{\Sigma}+\text{H.c.})-ig_{\Sigma\pi}\boldsymbol{\pi}\boldsymbol{\Sigma}\times\boldsymbol{\Sigma}+g_{\pi\Xi}\bar{\Xi}\boldsymbol{\tau}\Xi\cdot\boldsymbol{\pi}+g_{\Lambda K}(\bar{N}\Lambda K+\text{H.c.})+g_{\Sigma K}(\bar{N}\boldsymbol{\tau}\cdot\boldsymbol{\Sigma}K+\text{H.c.})$$
$$+h_{\Lambda K}(\bar{\Xi}\Lambda K^c+\text{H.c.})+h_{\Sigma K}(\bar{\Xi}\boldsymbol{\tau}\cdot\boldsymbol{\Sigma}K^c+\text{H.c.})+g_{N\eta}\bar{N}N\eta+g_{\Lambda\eta}\bar{\Lambda}\Lambda\eta+g_{\Sigma\eta}\boldsymbol{\Sigma}\cdot\boldsymbol{\Sigma}\eta+g_{\Xi\eta}\bar{\Xi}\Xi\eta\,,$$

where the field operators are given in the usual isospin notation, and

$$K_c=i\tau_2K^*=\begin{pmatrix}\bar{K}^0\\ -K^-\end{pmatrix}.$$

The coupling constants are related to $g_{N\pi}^2/4\pi=15$ by (in units of $g_{N\pi}$)

$$\begin{aligned}
&g_{N\pi}=1\,, && g_{\Lambda K}=-(1/\sqrt{3})(1+2f)\,, && g_{N\eta}=-(1/\sqrt{3})(1-4f)\,,\\
&g_{\Lambda\pi}=(2/\sqrt{3})(1-f)\,, && g_{\Sigma K}=(1-2f)\,, && g_{\Lambda\eta}=-(2/\sqrt{3})(1-f)\,,\\
&g_{\Sigma\pi}=2f\,, && h_{\Lambda K}=-(1/\sqrt{3})(1-4f)\,, && g_{\Sigma\eta}=(2/\sqrt{3})(1-f)\,,\\
&g_{\Xi\pi}=-(1-2f)\,, && h_{\Sigma K}=-1\,, && g_{\Xi\eta}=-(1/\sqrt{3})(1+2f)\,,
\end{aligned}$$

where the mixing parameter f is the ratio of F to D coupling.

(b) Pseudoscalar-Meson–Antibaryon–$D_{3/2}$-Octet Vertex

Same as in (a), where the operators, N, Λ, Σ, Ξ represent the $D_{3/2}$ resonances $N^{**}(1512)$, $\Lambda^{**}(1660)$, $\Sigma^{**}(1660)$, $\Xi^{**}(1810)$ and the mixing parameter has a different value, as discussed later.

(c) Pseudoscalar-Meson–Anti-$Y_0^*(1520)$-Singlet–Baryon Vertex

$$\mathfrak{L}^{SBP}=g_SY_0^*[\bar{K}N+\boldsymbol{\Sigma}\cdot\boldsymbol{\pi}+\Xi K+\Lambda\eta]+\text{H.c.}$$

(d) Pseudoscalar-Meson–Anti-Decuplet-Baryon Vertex

$$\mathcal{L}^{DBP}=g_D[\sqrt{2}\bar{N}_{3/2}^*(N\pi-\Sigma K)+(1/\sqrt{3})\bar{\mathbf{Y}}_1^*\cdot(\bar{K}\boldsymbol{\tau}N+\bar{K}^c\boldsymbol{\tau}\Xi-i\boldsymbol{\Sigma}\times\boldsymbol{\pi}-\sqrt{3}\Lambda\boldsymbol{\pi}+\sqrt{3}\boldsymbol{\Sigma}\eta)$$
$$+(1/\sqrt{3})\bar{\Xi}^*(\boldsymbol{\tau}\cdot\boldsymbol{\Sigma}K^c-\boldsymbol{\tau}\cdot\boldsymbol{\pi}\Xi+\sqrt{3}K^c\Lambda-\sqrt{3}\Xi\eta)+\sqrt{2}\bar{\Omega}^-\bar{K}\Xi]+\text{H.c.}$$

(e) Pseudoscalar-Meson–Vector-Meson–Pseudoscalar-Meson Vertex

$$\mathcal{L}^{PPV}=g_{\rho\pi}[\bar{\boldsymbol{\varrho}}\cdot\boldsymbol{\pi}\times\boldsymbol{\pi}+\tfrac{1}{2}i\sqrt{3}\bar{\varphi}K^*K+\tfrac{1}{2}i\bar{\boldsymbol{\varrho}}\cdot K^*\boldsymbol{\tau}K+\tfrac{1}{2}i\sqrt{3}\bar{K}^*K\eta+\tfrac{1}{2}i\bar{K}^*\boldsymbol{\tau}K\cdot\boldsymbol{\pi}-\tfrac{1}{2}i\sqrt{3}\bar{K}K^*\eta-\tfrac{1}{2}i\bar{K}\boldsymbol{\tau}K^*\cdot\boldsymbol{\pi}].$$

(f) Vector-Meson–Antibaryon–Baryon Vertex

Same as in (a), where the operators π, η, K, $\bar{K}$ represent the vector mesons, $\rho(750)$, $\varphi(1020)$, $K^*(890)$, $\bar{K}^*(890)$. The vector and tensor couplings each have different mixing parameters.

The relation between width and coupling constant was given in Sec. 4 for the special case of a state with $j=1+$. We list this relation for the $j=1-$, $2-$ states below:

$$j=1-:\quad g^2=\frac{\beta W_r^2\Gamma_r}{2q_r[(W_r-M)^2-m^2]},$$

$$j=2-:\quad g^2=\frac{\beta W_r^2\Gamma_r}{2q_r^3[(W_r-M)^2-m^2]}.$$

The factor β is proportional to the inverse of the product of the isotopic weight of the resonant state times the relevant $SU(3)$ coupling strength. The crossing table given above is normalized such that the proportionality constant determining $\beta=6$. The numerical values of these coupling constants taken from experimental values of widths and kinematical factors are given below.

$$g_{N\pi}^2/4\pi=15.0,\qquad g_D^2/4\pi=0.13,$$
$$g_S^2/4\pi=0.50,\qquad g_{D_{3/2}}^2/4\pi\ (\text{octet})=0.218,$$
$$g_{\rho N}{}^V g_{\rho\pi}/4\pi=3.0,\qquad g_{\rho N}{}^T g_{\rho\pi}/4\pi=-0.787.$$

We now give the crossing coefficients (isospin crossing coefficient times isotopic weight of exchange particle) first for u-channel exchange, then for t-channel exchange. The crossing elements are given by the notation (initial state, exchanged particle, final state).

u-Channel Exchange of Baryons

$S=1$, $T=0$: $3(NK,\Sigma,NK)-(NK,\Lambda,NK)$

$S=1$, $T=1$: $(NK,\Sigma,NK)+(NK,\Lambda,NK)$

$S=0$, $T=\frac{1}{2}$:

	$N\pi$	ΛK	ΣK	$N\eta$
$N\pi$	$-(N\pi,N,N\pi)$	$-\sqrt{3}(N\pi,\Sigma,\Lambda K)$	$2(N\pi,\Sigma,\Sigma K)+(N\pi,\Lambda,\Sigma K)$	$-\sqrt{3}(N\pi,N,N\eta)$
ΛK		$(\Lambda K,\Xi,\Lambda K)$	$+\sqrt{3}(\Lambda K,\Xi,\Sigma K)$	$(\Lambda K,\Lambda,N\eta)$
ΣK			$-(\Sigma K,\Xi,\Sigma K)$	$-\sqrt{3}(\Sigma K,\Sigma,N\eta)$
$N\eta$				$(N\eta,N,N\eta)$

$S=0$, $T=\frac{3}{2}$:

	$N\pi$	ΣK
$N\pi$	$2(N\pi,N,N\pi)$	$(N\pi,\Lambda,\Sigma K)-(N\pi,\Sigma,\Sigma K)$
ΣK		$2(\Sigma K,\Xi,\Sigma K)$

$S=-1$, $T=0$:

	$N\bar{K}$	$\Sigma\pi$	ΞK	$\Lambda\eta$
$N\bar{K}$	0	$-\sqrt{6}(N\bar{K},N,\Sigma\pi)$	$-(N\bar{K},\Lambda,\Xi K)+3(N\bar{K},\Sigma,\Xi K)$	$\sqrt{2}(N\bar{K},N,\Lambda\eta)$
$\Sigma\pi$		$(\Sigma\pi,\Lambda,\Sigma\pi)-2(\Sigma\pi,\Sigma,\Sigma\pi)$	$\sqrt{6}(\Sigma\pi,\Xi,\Xi K)$	$-\sqrt{3}(\Sigma\pi,\Sigma,\Lambda\eta)$
ΞK			0	$-\sqrt{2}(\Xi K,\Xi,\Lambda\eta)$
$\Lambda\eta$				$(\Lambda\eta,\Lambda,\Lambda\eta)$

$S=-1,\quad T=1$:

	$N\bar{K}$	$\Sigma\pi$	$\Lambda\pi$	ΞK	$\Sigma\eta$
$N\bar{K}$	0	$2(N\bar{K},N,\Sigma\pi)$	$-\sqrt{2}(N\bar{K},N,\Lambda\pi)$	$+(N\bar{K},\Lambda,\Xi K)+(N\bar{K},\Sigma,\Xi K)$	$-\sqrt{2}(N\bar{K},N,\Sigma\eta)$
$\Sigma\pi$		$(\Sigma\pi,\Sigma,\Sigma\pi)-(\Sigma\pi,\Lambda,\Sigma\pi)$	$+\sqrt{2}(\Sigma\pi,\Sigma,\Lambda\pi)$	$-2(\Sigma\pi,\Xi,\Xi K)$	$-\sqrt{2}(\Sigma\pi,\Sigma,\Sigma\eta)$
$\Lambda\pi$			$(\Lambda\pi,\Sigma,\Lambda\pi)$	$\sqrt{2}(\Lambda\pi,\Xi,\Xi K)$	$(\Lambda\pi,\Lambda,\Sigma\eta)$
ΞK				0	$\sqrt{2}(\Xi K,\Xi,\Sigma\eta)$
$\Sigma\eta$					$(\Sigma\eta,\Sigma,\Sigma\eta)$

$S=-1,\quad T=2$: $\quad(\Sigma\pi,\Sigma,\Sigma\pi)+(\Sigma\pi,\Lambda,\Sigma\pi)$

$S=-2,\quad T=\frac{1}{2}$:

	$\Xi\pi$	$\Lambda\bar{K}$	$\Sigma\bar{K}$	$\Xi\eta$
$\Xi\pi$	$-(\Xi\pi,\Xi,\Xi\pi)$	$-\sqrt{3}(\Xi\pi,\Sigma,\Lambda\bar{K})$	$2(\Xi\pi,\Sigma,\Sigma\bar{K})+(\Xi\pi,\Lambda,\Sigma\bar{K})$	$-\sqrt{3}(\Xi\pi,\Xi,\Xi\eta)$
$\Lambda\bar{K}$		$(\Lambda\bar{K},N,\Lambda\bar{K})$	$+\sqrt{3}(\Lambda\bar{K},N,\Sigma\bar{K})$	$(\Lambda\bar{K},\Lambda,\Xi\eta)$
$\Sigma\bar{K}$			$-(\Sigma\bar{K},N,\Sigma\bar{K})$	$-\sqrt{3}(\Sigma\bar{K},\Sigma,\Xi\eta)$
$\Xi\eta$				$(\Xi\eta,\Xi,\Xi\eta)$

$S=-2,\quad T=\frac{3}{2}$:

	$\Xi\pi$	$\Sigma\bar{K}$
$\Xi\pi$	$2(\Xi\pi,\Xi,\Xi\pi)$	$(\Xi\pi,\Lambda,\Sigma\bar{K})-(\Xi\pi,\Sigma,\Sigma\bar{K})$
$\Sigma\bar{K}$		$2(\Sigma\bar{K},N,\Sigma\bar{K})$

$S=-3,\quad T=0$: $\quad 3(\Xi\bar{K},\Sigma,\Xi\bar{K})-(\Xi\bar{K},\Lambda,\Xi\bar{K})$

$S=-3,\quad T=1$: $\quad(\Xi\bar{K},\Sigma,\Xi\bar{K})+(\Xi\bar{K},\Lambda,\Xi\bar{K})$

t-Channel Exchange

$S=1,\quad T=0$: $\quad 3(NK,\rho,NK)-(NK,\varphi,NK)$

$S=1,\quad T=1$: $\quad -(NK,\rho,NK)-(NK,\varphi,NK)$

$S=0,\quad T=\frac{1}{2}$:

	$N\pi$	ΛK	ΣK	$N\eta$
$N\pi$	$2(N\pi,\rho,N\pi)$	$\sqrt{3}(N\pi,\bar{K}^*,\Lambda K)$	$(N\pi,\bar{K}^*,\Sigma K)$	0
ΛK		$-(\Lambda K,\varphi,\Lambda K)$	$\sqrt{3}(\Lambda K,\rho,\Sigma K)$	$(\Lambda K,K^*,N\eta)$
ΣK			$-(\Sigma K,\varphi,\Sigma K)2(\Sigma K,\rho,\Sigma K)$	$-\sqrt{3}(\Sigma K,K^*,N\eta)$
$N\eta$				0

$S=0,\quad T=\frac{3}{2}$:

	$N\pi$	ΣK
$N\pi$	$-(N\pi,\rho,N\pi)$	$-2(N\pi,\bar{K}^*,\Sigma K)$
ΣK		$-(\Sigma K,\varphi,\Sigma K)-(\Sigma K,\rho,\Sigma K)$

$S=-1,\quad T=0$:

	$N\bar{K}$	$\Sigma\pi$	ΞK	$\Lambda\eta$
$N\bar{K}$	$3(N\bar{K},\rho,N\bar{K})+(N\bar{K},\varphi,N\bar{K})$	$\sqrt{6}(N\bar{K},\bar{K}^*,\Sigma\pi)$	0	$\sqrt{2}(N\bar{K},\bar{K}^*,\Lambda\eta)$
$\Sigma\pi$		$2(\Sigma\pi,\rho,\Sigma\pi)$	$\sqrt{6}(\Sigma\pi,\bar{K}^*,\Xi K)$	0
ΞK			$3(\Xi K,\rho,\Xi K)+(\Xi K,\varphi,\Xi K)$	$-\sqrt{2}(\Xi K,K^*,\Lambda\eta)$
$\Lambda\eta$				0

$S=-1,\quad T=1$:

	$N\bar{K}$	$\Sigma\pi$	$\Lambda\pi$	ΞK	$\Sigma\eta$
$N\bar{K}$	$-(N\bar{K},\rho,N\bar{K})+(N\bar{K},\varphi,N\bar{K})$	$-2(N\bar{K},\bar{K}^*,\Sigma\pi)$	$-\sqrt{2}(N\bar{K},\bar{K}^*,\Lambda\pi)$	0	$-\sqrt{2}(N\bar{K},\bar{K}^*,\Sigma\eta)$
$\Sigma\pi$		$(\Sigma\pi,\rho,\Sigma\pi)$	$-\sqrt{2}(\Sigma\pi,\rho,\Lambda\pi)$	$2(\Sigma\pi,\bar{K}^*,\Xi K)$	0
$\Lambda\pi$			0	$\sqrt{2}(\Lambda\pi,\bar{K}^*,\Xi K)$	0
ΞK				$-(\Xi K,\rho,\Xi K)\quad-(\Xi K,\varphi,\Xi K)$	$\sqrt{2}(\Xi K,K^*,\Sigma\eta)$
$\Sigma\eta$					0

$S=-1,\quad T=2$: $\quad -(\pi\Sigma,\rho,\pi\Sigma)$

$S=-2,\quad T=\frac{1}{2}$:

	$\Xi\pi$	$\Lambda\bar{K}$	$\Sigma\bar{K}$	$\Xi\eta$
$\Xi\pi$	$2(\Xi\pi,\rho,\Xi\pi)$	$-\sqrt{3}(\Xi\pi,K^*,\Lambda\bar{K})$	$-(\Xi\pi,K^*,\Sigma\bar{K})$	0
$\Lambda\bar{K}$		$(\Lambda\bar{K},\varphi,\Lambda\bar{K})$	$\sqrt{3}(\Lambda\bar{K},\rho,\Sigma\bar{K})$	$(\Lambda\bar{K},\bar{K}^*,\Xi\eta)$
$\Sigma\bar{K}$			$2(\Sigma\bar{K},\rho,\Sigma\bar{K})+(\Sigma\bar{K},\varphi,\Sigma\bar{K})$	$-\sqrt{3}(\Sigma\bar{K},\bar{K}^*,\Xi\eta)$
$\Xi\eta$				0

$S=-2,\quad T=\frac{3}{2}$:

	$\Xi\pi$	$\Sigma\bar{K}$
$\Xi\pi$	$-(\Xi\pi,\rho,\Xi\pi)$	$-2(\Xi\pi,K^*,\Sigma\bar{K})$
$\Sigma\bar{K}$		$-(\Sigma\bar{K},\varphi,\Sigma\bar{K})-(\Sigma\bar{K},\rho,\Sigma\bar{K})$

$S=-3,\quad T=0$: $\quad 3(\Xi\bar{K},\rho,\Xi\bar{K})+(\Xi\bar{K},\varphi,\Xi\bar{K})$

$S=-3,\quad T=1$: $\quad -(\Xi\bar{K},\rho,\Xi\bar{K})+(\Xi\bar{K},\varphi,\Xi\bar{K})$.

The u-channel elements for the exchange of the baryonic excited states are just those of the relevant baryons when possible, e.g., the crossing coefficients for $N^{**}(1512)$ are exactly those of $N(938)$. The only exchanged states which we use in this paper for which the crossing coefficients have not been given are $N^*(1238)$ and $\Omega^-(1676)$. These are listed below.

$S=0,\quad T=\frac{1}{2}$: $\quad \frac{4}{3}(N\pi,N^*(1238),N\pi)$

$S=0,\quad T=\frac{3}{2}$: $\quad \frac{1}{3}(N\pi,N^*(1238),N\pi)$

$S=-1,\quad T=0$: $\quad -\frac{2}{3}(\sqrt{6})(N\bar{K},N^*(1238),\Sigma\pi)$
$\quad -(\Xi K,\Omega^-,\Xi K)$

$S=-1,\quad T=1$: $\quad -\frac{2}{3}(N\bar{K},N^*(1238),\Sigma\pi)$
$\quad (\Xi K,\Omega^-,\Xi K)$

$S=-2,\quad T=\frac{1}{2}$: $\quad \frac{4}{3}(\Sigma\bar{K},N^*(1238),\Sigma\bar{K})$

$S=-2,\quad T=\frac{3}{2}$: $\quad \frac{1}{3}(\Sigma\bar{K},N^*(1238),\Sigma\bar{K})$.

Finally, we give the transformation, relating $SU(3)$ multiplets to two particle meson-baryon states, which we used in our calculations. We use the notation $|IR\rangle_T{}^Y$ where Y is the hypercharge and T is the isospin

$$|\mathbf{27}\rangle_1{}^2 = KN,$$
$$|\mathbf{27}\rangle_{3/2}{}^1 = -(1/\sqrt{2})[N\pi+\Sigma K],$$
$$|\mathbf{27}\rangle_{1/2}{}^1 = (20)^{-1/2}[3N\eta+3\Lambda K-\Sigma K-N\pi],$$
$$|\mathbf{27}\rangle_1{}^0 = (10)^{-1/2}[-\sqrt{2}N\bar{K}-\sqrt{3}\Lambda\pi-\sqrt{3}\Sigma\eta-\sqrt{2}\Xi K],$$
$$|\mathbf{27}\rangle_0{}^0 = [2(30)^{1/2}]^{-1}[+9\Lambda\eta-\sqrt{3}\Sigma\pi-3\sqrt{2}N\bar{K}+3\sqrt{2}\Xi K],$$
$$|\mathbf{27}\rangle_{3/2}{}^{-1} = (1/\sqrt{2})[\Sigma\bar{K}+\Xi\pi],$$
$$|\mathbf{27}\rangle_{1/2}{}^{-1} = (20)^{-1/2}[-\Xi\pi-\Sigma\bar{K}-3\Xi\eta-3\Lambda\bar{K}],$$
$$|\mathbf{27}\rangle_1{}^{-2} = \Xi\bar{K},$$
$$|\mathbf{27}\rangle_2{}^0 = \Sigma\pi,$$
$$|\mathbf{10}\rangle_{3/2}{}^1 = (1/\sqrt{2})[N\pi-\Sigma K],$$
$$|\mathbf{10}\rangle_1{}^0 = \tfrac{1}{2}[\Lambda\pi-\Sigma\eta+(\tfrac{2}{3})^{1/2}N\bar{K}-(\tfrac{2}{3})^{1/2}\Xi K+(\tfrac{2}{3})^{1/2}\Sigma\pi],$$
$$|\mathbf{10}\rangle_{1/2}{}^{-1} = \tfrac{1}{2}[-\Xi\eta+\Lambda\bar{K}+\Xi\pi-\Sigma\bar{K}],$$
$$|\mathbf{10}\rangle_0{}^{-2} = \Xi\bar{K},$$
$$|8_S\rangle_{1/2}{}^1 = (1/2\sqrt{5})[-3N\pi-\Lambda K-3\Sigma K-N\eta],$$
$$|8_S\rangle_0{}^0 = (1/\sqrt{5})[-\Lambda\eta-\sqrt{3}\Sigma\pi-(1/\sqrt{2})N\bar{K}+(1/\sqrt{2})\Xi K],$$
$$|8_S\rangle_1{}^0 = (10)^{-1/2}[-\sqrt{2}\Sigma\eta-\sqrt{2}\Lambda\pi+\sqrt{3}N\bar{K}+\sqrt{3}\Xi K],$$
$$|8_S\rangle_{1/2}{}^{-1} = = (1/2\sqrt{5})[\Xi\eta+\Lambda\bar{K}-3\Sigma\bar{K}-3\Xi\pi],$$
$$|8_A\rangle_{1/2}{}^1 = \tfrac{1}{2}[N\eta-\Lambda K-N\pi+\Sigma K],$$
$$|8_A\rangle_1{}^0 = (1/\sqrt{6})[-N\bar{K}+2\Sigma\pi+\Xi K],$$
$$|8_A\rangle_0{}^0 = (1/\sqrt{2})[-N\bar{K}-\Xi K],$$
$$|8_A\rangle_{1/2}{}^{-1} = \tfrac{1}{2}[\Xi\eta-\Lambda\bar{K}+\Xi\pi-\Sigma\bar{K}],$$
$$|1\rangle_0{}^0 = (1/2\sqrt{2})[-\Lambda\eta+\sqrt{3}\Sigma\pi-\sqrt{2}N\bar{K}+\sqrt{2}\Xi K],$$
$$|\overline{\mathbf{10}}\rangle_0{}^2 = NK,$$
$$|\overline{\mathbf{10}}\rangle_{1/2}{}^1 = \tfrac{1}{2}[\Lambda K-N\eta-N\pi+\Sigma K],$$
$$|\overline{\mathbf{10}}\rangle_1{}^0 = \tfrac{1}{2}[\Sigma\eta-\Lambda\pi+(\tfrac{2}{3})^{1/2}N\bar{K}-(\tfrac{2}{3})^{1/2}\Xi K+(\tfrac{2}{3})^{1/2}\Sigma\pi],$$
$$|\overline{\mathbf{10}}\rangle_{3/2}{}^{-1} = (1/\sqrt{2})[\Xi\pi-\Sigma\bar{K}].$$